



Damage Tolerance Capacity of Exterior Beam-Column Joint with High-Performance Fiber Reinforced Cementitious Composite

Nikhil R. Jadhav^{1,2}(✉) and R. Siva Chidambaram²

¹ School of Civil Engineering, Vellore Institute of Technology, Vellore 632014, India
nikhil8255@gmail.com

² CSIR-Central Building Research Institute, Roorkee 247667, India

Abstract. The shear resistance behavior of beam-column joint decides the ductile performance of the reinforced concrete (RC) framed structure. The brittle nature of concrete fails to resist the alternate diagonal compression and tension at the joint region and leads to shear failure. The use of closely spaced stirrups at the plastic hinge region of the joints leads to construction difficulty and works up to a certain extent in providing ductility. The use of discontinuous steel fiber in concrete (SFRC) is one of a kind to improve the joint shear resistance. But the higher volume of steel fiber leads to fiber balling and workability issues which restricts the efficiency of SFRC in joint shear resistance. The absence of coarse aggregate and presence of fine mineral admixtures in high performance fiber reinforced cementitious composites (HPFRCC) overcome the issues with SFRC and enhances the ductility and damage tolerance of joint. In this study the HPFRCC is used at the joint region without critical detailing and tested under reverse cyclic loading. The presence of 1% synthetic fiber and better fiber dispersion improves the crack bridging ability of HPFRCC and allows dense micro cracks formation at the hinge region. The hysteresis curve shows improved shear strength and the post failure analysis shows that the formation of multiple micro cracks enhances the displacement ductility. The use of HPFRCC in the joint region eliminates the need of seismic detailing without compromising the shear resistance and eases the construction activity with improved ductility.

Keywords: HPFRCC · Exterior beam-column joints · Cyclic loading · Damage tolerance · AJI2010 · IS-13920:2016

1 Introduction

Beam column joints have vital role of transferring forces from beam and column to foundation. During earthquake, joints experience huge amount of shear forces, these forces are resisted by strut and tie mechanism. The brittle nature of concrete commonly fails by bond slipping, concrete spalling and brittle shear failure. There are two major ways to increase the shear strength of joint, one is to provide adequate shear reinforcement which helps to provide confinement to core concrete, and another way is to increase performance of concrete in joint region and probable plastic hinge region. But additional shear

reinforcement in the joint region causes congestion in joint area and creates construction difficulties. In past few decades various innovative research using different confinement ratio, steel fiber reinforced concrete (SFRC), external strengthening using reinforced concrete (RC) jacketing has been carried out to increase the shear capacity of joint. The use randomly distributed steel fiber in concrete helps to enhance the performance of concrete by fiber crack bridging action and early crack resistance mechanism. Performance of SFRC mainly depends of fiber volume and properties of steel fibers. Steel fibers increases mechanical properties of concrete like compression, bending, tensile strength, toughness. Use of SFRC in beam-column joint have resulted in enhanced ductility, shear resistance and energy dissipation and acts as secondary transverse reinforcement (Jiuru et al. 1992). Increased percentage of steel fiber creates workability issues and creates problems like fiber balling, honey combing therefore it is limited to 2–3%. To eliminate the limitations of SFRC, High Performance Fiber Reinforced Cementous Composites (HPFRCC) is emerged. In HPFRCC coarse aggregates are replaced by various types of fibers such as polymer, steel, carbon etc... and mineral admixtures such as fly ash, silica fume, ground granulated blast furnace slags etc. Proper distribution of fibers and absence of coarse aggregate provides strain hardening properties. HPFRCC are more ductile than conventional concrete and SFRC. HPFRCC possess strain hardening and fine multiple cracking characteristics under tension. The toughness behavior of HPFRCC prevents crushing and spalling of concrete and allows the rebar to yield and exhibits ductile failure with improved energy dissipation.

According to Li et al. (2003) HPFRCC have multiple cracking and strain hardening characteristics in tension along with enhanced ductile properties. Chao et al. (2009) conducted experiments to study bond behavior and tensile properties of HPFRCC, observation from test shows that fiber bridging provides post cracking strength and limits crack width this leads to enhanced bond strength. HPFRCC also shows damage control ability and stiffness retention capacity. Parra-Montesinos et al. (2009) conducted study on interior beam column joint with HPFRCC and observed that joints have higher damage tolerance capacity and allowed to increase spacing of transverse reinforcement. Yuan et al. (2013) investigated beam column joints with ECC. Results shows that ECC shows improvement in ductility and load capacity and additional axial load limits propagation on cracks in joint core. Fakharifar et al. (2014) Extensively investigated mechanical properties of HPFRCC such as compression, bending and impact and proposed equation's and also observed that increased fiber percentage increases number of blow count. Chidambaram et al. (2015) investigated effect of HPFRCC in beam column joint and use of HPFRCC in joint resulted in change of failure pattern to ductile and Joint with HPFRCC can be 2 to 3 times more ductile than normal concrete with widely spread crack at joint and minor cracks in beam and joint region. Li et al. (2017) used HPFRCC for retrofitting of column, ductility of repaired columns was 29% and load carrying capacity was 14% of original column. Saghaf et al. (2019) investigated feasibility of HPFRCC in beam column joint for seismic loading. Joint remained intact without any cracks this implies shear requirements satisfies without any transverse reinforcement.

Research Significance

Many experimental studies have been carried out to highlight the damage tolerance and efficiency of HPFRCC in beam column joint. Very limited research has been done to

predict shear strength of joint with HPFRCC. Available codes are unable to predict the HPFRCC joint shear strength. Based on type of fibers used in composite, modification factors have been proposed for IS 13920:2016 and AJI-2010 and validated using the experimental data and data from various literatures.

2 Experimental Program and Materials

An experimental study is carried out to study the effect of ECC with moderate confinement in the beam-column joint hinge region. Mix ratio of concrete and composites are given in Table 1.

Table 1. Mix ratio of concrete & composites

Specimen ID	Cement	Fine aggregate	Coarse aggregate	Fly ash	Water Binder ratio
Normal concrete	1	1.55	5.27	–	0.45
HPFRCC-1	1	0.75	–	0.25	0.33

Cylindrical specimens with 100 mm diameter and 200 mm height have been cast and tested under uniaxial compression testing. The compressive strength of the different composites is shown in Table 3. Two exterior joint specimens, one with normal concrete and another with 1% polypropylene fiber based ECC are constructed and tested under quasi-static loading. HPFRCC composite was placed in the plastic hinge region as shown in Fig. 2. A schematic illustration of the experimental test setup is presented in Fig. 1. and reinforcement details are given in Table 2 Joints were without seismic detailing prepared as per design recommendations of IS 456–2000, cyclic loading protocol is provided as per FEMA 461 loading protocol (Fig. 3).

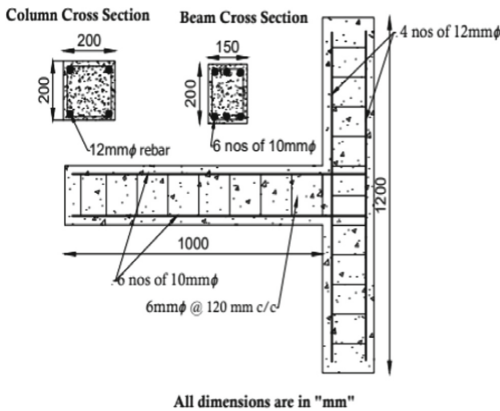


Fig. 1. Reinforcement details.

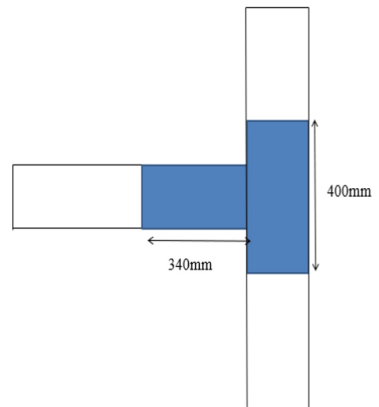


Fig. 2. Location of HPFRCC in joint.

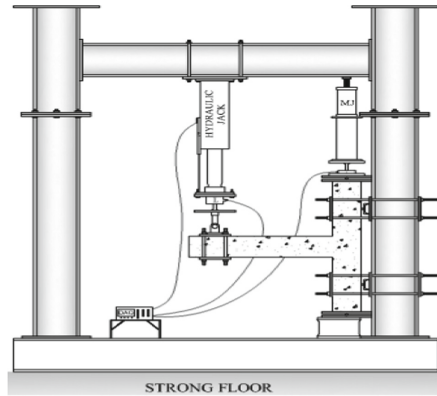


Fig. 3. Test setup.

Table 2. Reinforcement details

Specimen ID	Beam reinforcement	Column reinforcement	Transverse reinforcement
NC HPFRCC	All specimens are reinforced with 3Φ10 at top and bottom (ratio = 1.57%)	All specimens are reinforced with 4Φ12 (ratio = 1.97%)	All specimens with Φ6@100 mm in column and Φ6@120 mm in beam

Table 3. Compressive strength

Specimen ID	Polypropylene Fibers %	Steel fibers (%)	Cylinder Compression Test (MPa)
Normal concrete	–	–	20
HPFRCC-1	1%	–	23

3 Results and Discussion

3.1 Failure Mode and Crack Propagation

Figure 4 shows crack pattern of both specimens at the final stage. The first crack was observed at 22 mm away from the face of the column in the plastic hinge region of conventional specimen NC. The first crack load was of 21.6 kN with drift ratio of 1%. Later as the test proceeded, cracks are formed within the beam plastic hinge regions from the face of the column. A peak load of 30 kN at the drift ratio of 2.83% was observed. At 5% drift crushing of concrete started, as shown in Fig. 4. Brittle failure with crushing of concrete and buckling of reinforcement were observed. Failure was shifted to local failure because of the higher stiffness of the column than a beam, but the absence of adequate confinement in the hinge region failed to restrict the rebar buckling.

In HPFRCC specimen the first crack was observed at 20 mm away from the face of a column in the plastic hinge region and at a load of 28.1 kN which is 30% more than NC with a drift ratio of 1%. Cracks were formed in the region of 400 mm from the face of the column. The type of failure of HPFRCC is changed from brittle failure to ductile failure due to high ductile and damage tolerance characteristics of ECC. It is also noticed that HPFRCC joint experienced numerous micro cracks instead of single primary crack. HPFRCC shows one wide crack at joint interface and fine cracks in beam. The lesser volume PP fiber based ECC failed to arrest the rebar slippage which shows longitudinal reinforcement slip at the back side of column as shown in Fig. 4.

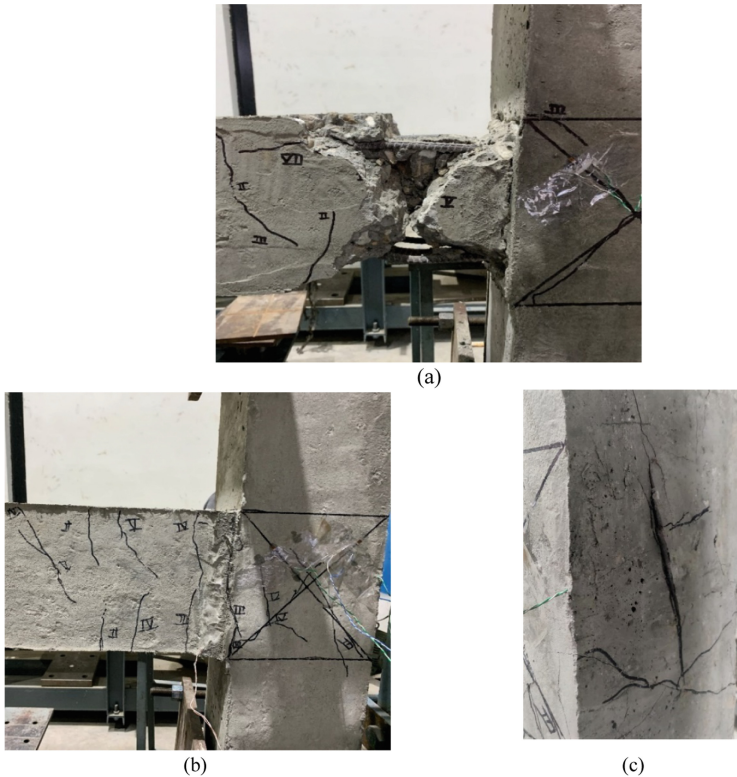


Fig. 4. (a) crack pattern for normal concrete (b) crack pattern for HPFRCC (c) Pull-out crack at the back of the column of HPFRCC specimen.

3.2 Hysteresis Behavior

Hysteresis Responses of both NC and HPFRCC specimens are shown in Fig. 5, and Table 4 summarizes first crack characteristics and ultimate load and displacement values. It is noted that HPFRCC has shown an increase in ultimate load and ultimate displacement. Ultimate load is increased by nearly 10% and maximum drift by 50%. After peak load,

NC experiences sudden drop in load capacity whereas in HPFRCC shows stable and gradually decrease in load as drift increases. Shear resistance of HPFRCC is 30% higher than normal concrete. Figure 6 shows the load-deformation envelop over displacement of NC and HPFRCC specimens. The curve shows that the yield strength of the HPFRCC is higher than NC. Yield strength is assumed to be 0.8 times of peak load, and the displacement corresponding to displacement of initial stiffness line at load 0.8 times peak is yield displacement. Ductility is a ratio of ultimate displacement to yield displacement. HPFRCC shows 50% higher displacement ductility as a result of larger rotation compared to NC.

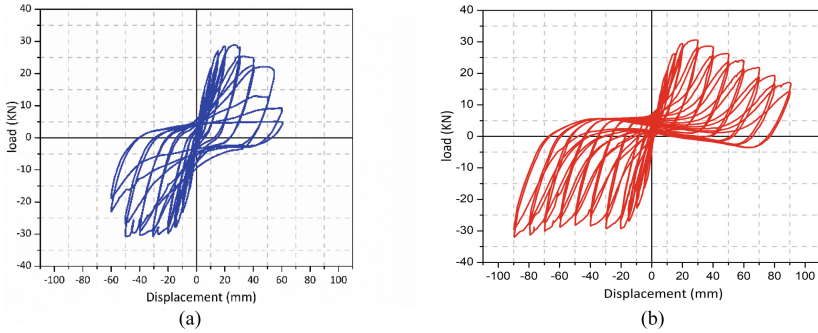


Fig. 5. (a) Hysteresis loop of normal concrete (b) Hysteresis loop of for HPFRCC.

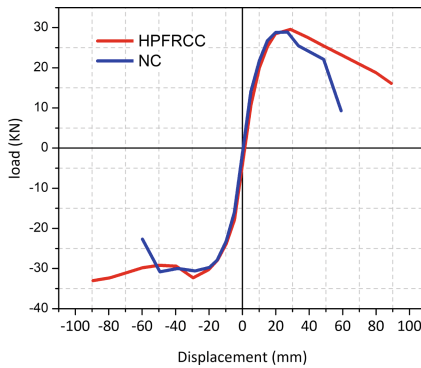


Fig. 6. Load displacement envelop.

3.3 Energy Dissipation

The amount of energy absorbed is an area enclosed by loops of hysteresis curve. The longitudinal rebar slip at early stage of HPFRCC shows pinching in the hysteresis curve. Thus, the HPFRCC shows gradual increase in energy dissipation compared to NC. The observed cumulative energy dissipation (CED) of HPFRCC at failure is 40% larger

Table 4. Result of test specimen

Specimen ID	Frist crack load	Frist crack drift (%)	Maximum drift (%)	Ultimate load(kN)		Maximum load (kN)		Ductility $\Delta u/\Delta y$
				Positive	Negative	Positive	Negative	
NC	21.6	1	6	28.9	-30.8	9.3	-22.7	3.05
HPFRCC	22.5	1	9	29.6	-33	16.1	-33	4.77

than NC. Until 3% drift NC and HPFRCC dissipates same energy, but after 3% energy dissipation of HPFRCC declines, and pinching is observed hence, after 3% no new cracks has been observed and therefore, HPFRCC after 3% of drift fibers prevent widening of cracks by fiber bridging action. This authenticates the efficacy of the ECC in dissipating the energy even with lesser compressive strength (Figs. 7, 8).

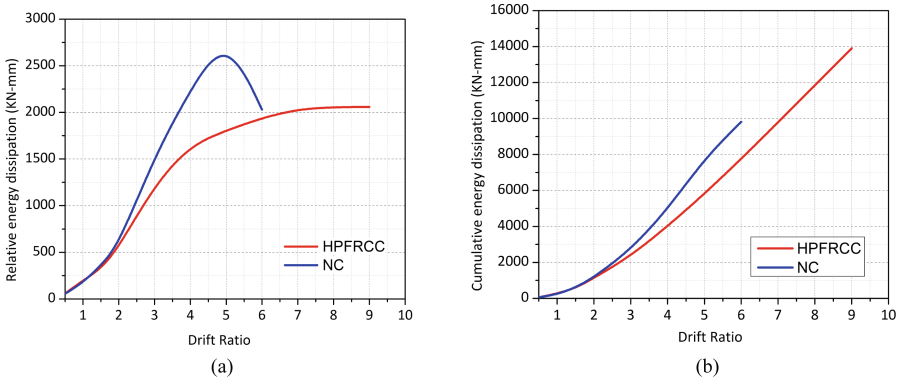


Fig. 7. (a) Relative energy dissipation (b) cumulative energy dissipation.

3.4 Stiffness Behavior

The tangent to the initial load – deflection curve shows the Initial stiffness of joint specimens. The initial stiffness of HPFRCC is 1.6 times higher than NC, whereas the post peak stiffness decreases rapidly in NC compared to HPFRCC. Yield stiffness is ratio of yield load to yield displacement. Fiber bridging action of HPFRCC provides 1.2 times higher yield stiffness than NC. The rate of change in degradation is more in NC than in HPFRCC which shows brittle failure and a lower rate of stiffness reduction in HPFRCC shows ductile failure. At 6% drift HPFRCC shows 60% more stiffness than NC (Fig. 9).

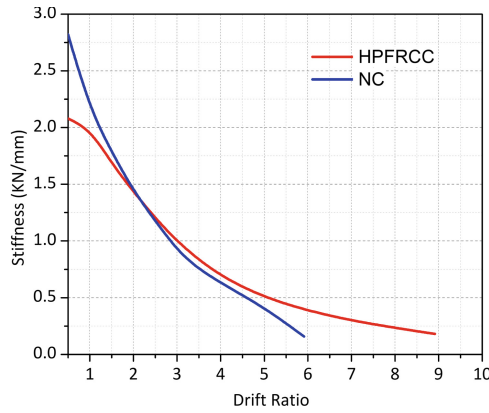


Fig. 8. Stiffness over drift ratio.

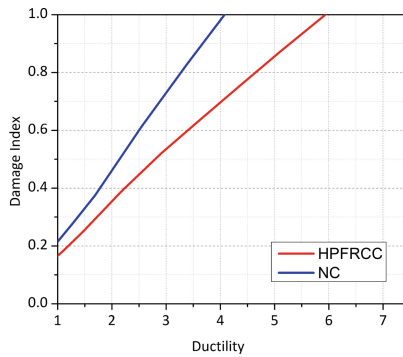


Fig. 9. Damage index over ductility.

3.5 Damage Index

According to Park et al. (1985). damage index is

$$D = \frac{\delta m}{\delta u} + \frac{\beta}{\delta u F_y} \int dE \tag{1}$$

“Δm” is Maximum displacement under earthquake or cyclic, “δu” is ultimate deformation, “Fy” is yield strength of beam-column joint, β is strength reduction factor, for RC structure it is 0.1 Villemure (1993). DI varies from 1 to 0. As the value increases damage increases, 0 means no damage, and 1 is complete damage. It can be seen from the graph that HPFRCC has more damage tolerance than normal concrete for all levels. HPFRCC shows 70% damage when NC is completely damaged. The ductile failure behavior of HPFRCC shows 30% higher damage tolerant than NC even without critical confinement. Also, the absence of rebar buckling without critical confinement shows the efficacy of the HPFRCC confinement action and damage tolerance.

4 Joint Shear Strength Criteria for Building Codes

The joint shear strength as per Indian and Japan standards are given in the Table for IS-13920:2016 and AIJ:2010 (Table 5).

Table 5. Code provision for shear strength of joint

Code of practice	Joint Shear
IS-13920:2016	$\Phi\sqrt{f_c A_j}$
AIJ:2010	$\Phi\eta F_j A_j$

η represents shape factor for joints as 0.70, 1.00, and 0.40 for exterior, interior, and knee joints. f_c is concrete cube compressive strength for IS code. F_j represents a concrete factor in AJI-2010. confinement factor Φ from code is given in the Table 6.

Table 6. Values of confinement factor Φ for IS and AJI.

	IS-13920:2016	AIJ:2010
All four sides	1.5	1
Three or two sides	1.2	0.85
Other cases	1	0.85

Shear strength of the beam-column joint is based on various factors such as normalized column axial stress, beam bars index, normalized vertical joint shear reinforcement, normalized horizontal joint shear reinforcement, and most important is the compressive strength of concrete Tran (2016). But in code recommendations, only compressive strength is considered as a major factor; therefore, codes are unable to predict shear strength of HPCRCC perfectly. Following factors are proposed especially for HPCRCC for different types of fiber used in composite and it has resulted in increased efficiency of code provisions. Factors are given in Table 7 and mean, standard deviation, and covariance of V_j experimental/ V_j code is given in Table 8 with R2 and slope of trendline of V_j experimental vs V_j code graphs. Brief database is summarized in Annexure A.

Table 7. Modification factor

Category	IS-13920:2016	AJI-2010
Hybrid	0.7	0.6
Steel fiber	0.8	0.7
ECC	0.6	0.75

Table 8. Comparison of code recommendation and modified.

	IS-13920:2016	Modified IS-13920:2016	AJI-2010	Modified AJI 2010
Average value	0.675	1.07	0.6721	0.988
SD	0.086	0.157	0.0937	0.165
Covariance	0.12	0.146	0.1394	0.165
Slope	1.42	0.88	1.448	1.09
R ²	0.98	0.97	0.97	0.9

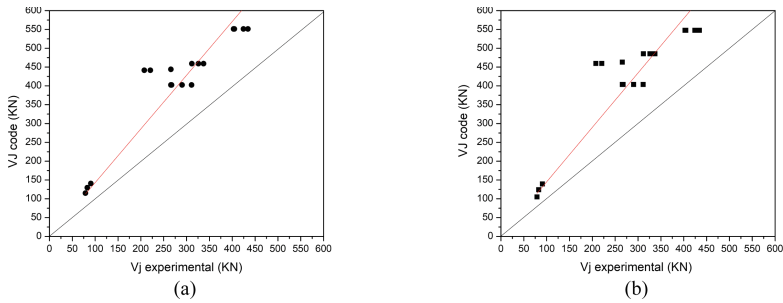


Fig. 10. Comparison of code predicted joint shear strength with experimental database without modification factor (a) IS-13920:2016 (b) AJI 2010.

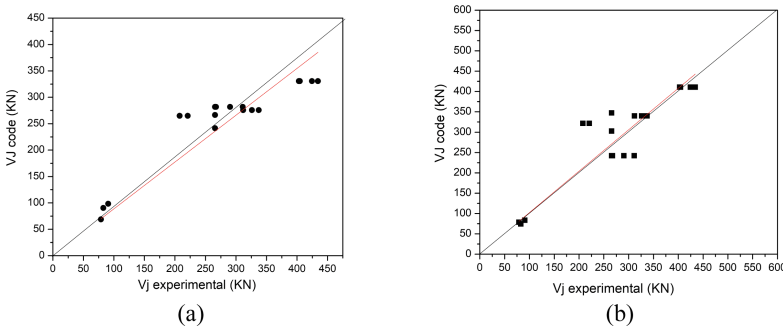


Fig. 11. Comparison of code predicted joint shear strength with experimental database with modification factor (a) modified IS-13920:2016, (b) modified AJI-2016.

Figure 10 shows comparisons between IS-13920:2016 and AJI-2010 code prediction of shear strength of beam column joints with HPFRCC and Fig. 11 shows modified shear strength model for HPFRCC beam column joint. The shear strength mean is 0.675 and 0.672 respectively for IS and AIJ models with a slope of 1.42 and 1.448 respectively. Figure 11 shows efficiency of the proposed model in estimating the joint shear strength

of HPFRCC. It shows a mean value of 1.07 and 0.98 for modified IS 13920:2016 and AJI 2010. The Slope of trendline is 0.88 and 1.09 respectively which is 23.86% better than the actual model. The validation shows that the modification factors proposed are more effective in estimating the joint shear strength of HPFRCC using various fibers.

5 Conclusion

In this study, two joints have been tested under cyclic loading to investigate damage tolerance of HPFRCC over normal concrete. Both of the joints prepared with moderate transverse reinforcement.

- 1) HPFRCC shows improvement over failure pattern, both specimens failed in plastic hinge region of beam with minor cracks in core of joint. Normal concrete crush and reinforcement bar was bended but in HPFRCC wide crack forms at the face of column but no bending or rupture of reinforcement noticed.
- 2) Damage index of HPFRCC is lower than normal concrete, Normal concrete reaches ductility level of 4, and HPFRCC reaches to level 7. This proves that joint with HPFRCC have more damage tolerance than normal concrete.
- 3) Relative and cumulative energy dissipation is calculated using enclosed loop area. Average cumulative energy dissipation of HPFRCC is 1.4 times more than normal concrete at 9% drift ratio.
- 4) Initial and yield stiffness of HPFRCC is 1.2 and 1.6 times higher than normal concrete due to effective fiber bridging action.
- 5) Building Codes are unable to predict correct shear strength of joint for HPFRCC joints, statistical analysis shows that proposed modification factors efficiently improve accuracy of IS 13920:2016 and AJI 2010.

Appendix-A

Sr. No.	Year	Specimen ID	Beam properties				column Properties				% Volume at joint		CATEGORY	Vj horizontal Experimental	Vj IS modified	Vj AI modified	
			Bb	Hb	Ast	Bc	Hc	Ast	Fc'	PP /PVA	SF						
R. Siva Chidambaram et al. 2015																	
1	2015	S/4	130	150	471.23	150	150	452.3	26	3	3	SYNTHETIC	78.81	114.728	68.83	104.77	78.58
2	2015	S/5	130	150	471.23	150	150	452.3	39	1.5	2	HYBRID	90.63	140.512	98.35	139.16	83.49
3	2015	S/6	130	150	471.23	150	150	452.3	33	1.5	2	HYBRID	82.75	129.253	90.47	123.80	74.28
Mohammad hossein Saghafi et al. (2018)																	
J1-C1-																	
4	2018	HPFRCC	220	250	1231.5	250	250	1231	41.47	1	1	HYBRID	290.3	402.483	281.738	403.55	242.1
J1-C2-																	
5	2018	HPFRCC	220	250	1231.5	250	250	1231	41.47	1	1	HYBRID	311.0	402.483	281.738	403.55	242.1
J2-C1-																	
6	2018	HPFRCC	220	250	1231.5	250	250	1231	41.47	1	1	HYBRID	267.3	402.483	281.738	403.55	242.1
J2-C2-																	
7	2018	HPFRCC	220	250	1231.5	250	250	1231	41.47	1	1	HYBRID	265.6	402.483	281.738	403.55	242.1
Mohammad hossein Saghafi et al. (2020)																	
ECC-STEEL																	
8	2020	J2HP1	220	250	1077.5	250	250	123	49.92	2	2	FIBER	207.7	264.95	353.27	459.49	321.6
ECC-STEEL																	
9	2020	J2HP2	220	250	1077.5	250	250	1231	49.92	2	2	FIBER	220.8	264.95	353.27	459.49	321.6
Mohammad hossein Saghafi et al. (2019)																	
ECC-																	
10	2019	SC2-A	220	250	1077.5	250	250	1231	41.47	1	1	SYNTHETIC	265.6	402.483	241.49	403.55	302.6
ECC-STEEL																	
11	2019	SC2-B	220	250	1077.5	250	250	1231.5	50.47	2	2	FIBER	265.6	444.014	266.41	463.03	347.2

Mohammad hossein Saghafi et al. (2021)																
12	2021	BCI2-HPC	220	250	1077.7	250	250	1231.5	54	ECC-STEEL	2	311.6	459.279	275.57	485.47	339.8
										FIBER						
13	2021	BCI3-HPC	220	250	1077.5	250	250	1231.5	54	ECC-STEEL	2	337.2	459.279	275.57	485.47	339.8
										FIBER						
14	2021	BCI4-HPC	220	250	1077.5	250	250	1231.5	54	ECC-STEEL	2	326.0	459.279	275.57	485.47	339.8
										FIBER						
Fang Yuan et al(2011)																
15	2011	S3	200	400	1884.9	250	350	1256.64	39.68	ECC-SYNTHETIC		402.9	551.181	330.708	547.79	410.8
										ECC-SYNTHETIC						
16	2011	S4	200	400	1884.9	250	350	1256.64	39.68	ECC-SYNTHETIC		434.4	551.181	330.708	547.79	410.8
										ECC-SYNTHETIC						
17	2011	S5	200	400	1884.9	250	350	1256.64	39.68	ECC-SYNTHETIC		424.5	551.181	330.708	547.79	410.8
										ECC-SYNTHETIC						
18	2011	S6	200	400	1884.9	250	350	1256.64	39.68	ECC-SYNTHETIC		404.6	551.181	330.708	547.79	410.8
										ECC-SYNTHETIC						

References

- Architectural Institute of Japan (AIJ): AIJ standard for structural calculation of reinforced concrete structures (Japanese). Maruzen, Tokyo (2010)
- Chao, S.H., Naaman, A.E., Parra-Montesinos, G.J.: Bond behavior of reinforcing bars in tensile strain-hardening fiber-reinforced cement composites. *ACI Struct. J.* **106**(6), 897 (2009)
- Chidambaram, R.S., Agarwal, P.: Seismic behavior of hybrid fiber reinforced cementitious composite beam–column joints. *Mater. Des.* **86**, 771–781 (2015)
- Fakharifar, M., Dalvand, A., Arezoumandi, M., Sharbatdar, M.K., Chen, G., Kheyroddin, A.: Mechanical properties of high performance fiber reinforced cementitious composites. *Constr. Build. Mater.* **71**, 510–520 (2014)
- Saghafi, M.H., Shariatmadar, H.: Enhancement of seismic performance of beam-column joint connections using high performance fiber reinforced cementitious composites. *Constr. Build. Mater.* **180**, 665–680 (2018)
- Villemure, I.: Damage Indices for Reinforced Concrete Frames Evaluation and Correlation (Master of Applied Science Thesis) The University of British Columbia (1993)
- IS 13920: Ductile design and detailing of reinforced concrete structures subjected to seismic forces Code of practice, India (2016)
- Jiuru, T., Chaobin, H., Kaijian, Y., Yongcheng, Y.: Seismic behavior and shear strength of framed joint using steel-fiber reinforced concrete. *J. Struct. Eng.* **118**(2), 341–358 (1992)
- Li, V.C.: On engineered cementitious composites (ECC) a review of the material and its applications. *J. Adv. Concr. Technol.* **1**(3), 215–230 (2003)
- Li, X., Wang, J., Bao, Y., Chen, G.: Cyclic behavior of damaged reinforced concrete columns repaired with high-performance fiber-reinforced cementitious composite. *Eng. Struct.* **136**, 26–35 (2017)
- Parra-Montesinos, G.J., Peterfreund, S.W., Shih-Ho, C.: Highly damage-tolerant beam-column joints through use of high-performance fiber-reinforced cement composites. *ACI Struct. J.* **102**(3), 487 (2005)
- Park, Y.J., Ang, A.H.S.: Mechanistic seismic damage model for reinforced concrete. *J. Struct. Eng.* **111**(4), 722–739 (1985)
- Patel, P.A., Desai, A.K., Desai, J.A.: Evaluation of RC and SFRC exterior beam–column joint under cyclic loading for the reduction in lateral reinforcement of the joint region. *Mag. Concr. Res.* **65**(7), 405–414 (2013)
- Villemure, S.: Damage Indices for Reinforced Concrete Frames Evaluation and Correlation (Master of Applied Science Thesis) The University of British Columbia (1993)
- Saghafi, M.H., Golafshar, A., Zareian, M.S., Kashani, M.: The effect of high-performance fiber-reinforced cementitious composites on the lateral behavior of reinforced concrete frames without seismic details. *Structures* **26**, 801–813. Elsevier (2020)
- Saghafi, M.H., Shariatmadar, H., Kheyroddin, A.: Seismic behavior of high-performance fiber-reinforced cement composites beam-column connection with high damage tolerance. *Int. J. Concr. Struct. Mater.* **13**(1), 1–20 (2019)
- Tran, M.T.: Influence factors for the shear strength of exterior and interior reinforced concrete beam-column joints. *Procedia Eng.* **142**, 63–70 (2016)
- Yuan, F., Pan, J., Xu, Z., Leung, C.K.Y.: A comparison of engineered cementitious composites versus normal concrete in beam-column joints under reversed cyclic loading. *Mater. Struct.* **46**(1), 145–159 (2013)